ACS APPLIED NANO MATERIALS

Article

Cite This: ACS Appl. Nano Mater. 2020, 3, 814−819

www.acsanm.org

# White-Light-Emitting Diodes from Directional Heat-Conducting Hexagonal Boron Nitride Quantum Dots

Shuling Zhou,[†] Yupu Ma,[†] Xinfeng Zhang,[†] Wei Lan,[†] Xingjian Yu,[†] Bin Xie,[†] Kai Wang,*[,‡] and Xiaobing Luo*[,†]

[†]State Key Laboratory of Combustion, School of Energy and Power Engineering, Huazhong University of Science and Technology, Wuhan 430074, China

[‡]Department of Electrical and Electronic Engineering, Southern University of Science and Technology, Shenzhen 518055, China

**ABSTRACT:** In quantum-dots-converted white-light-emitting diodes (QDs-WLEDs), red-emitting quantum dots are usually mixed with yellow-emitting phosphors in luminescent polymer layer to achieve a high color rendering index. However, the thermal stability of QDs is severely challenged by the high working temperature of the luminescent polymer layer with a low thermal conductivity. In this work, we enhanced the vertical thermal conductivity of the luminescent layer by filling vertically arranging hexagon boron nitride sheets (hBNS) inside using an ice template method. This created a relatively high thermal conductivity heat dissipation channel for luminescent particles. Sodium carboxymethylcellulose templates were created to support the vertically arranging hBNS. Using the proposed method, we fabricated a new package design of vertical-enhanced QDs-WLEDs (Ver-WLEDs) and compared its thermal performance with that of isotropic-enhanced QDs-WLEDs (Iso-WLEDs) and common QDs-WLEDs (Com-WLEDs). At the same working current, the maximal working temperature of Ver-WLEDs (116 °C) was 36 and 21 °C lower than that of Iso-WLEDs (152 °C) and Com-WLEDs (137 °C), respectively. Our novel method to enhance the vertical thermal conductivity of luminescent polymer layer could shed light on the application of QDs in high-power light-emitting diodes.

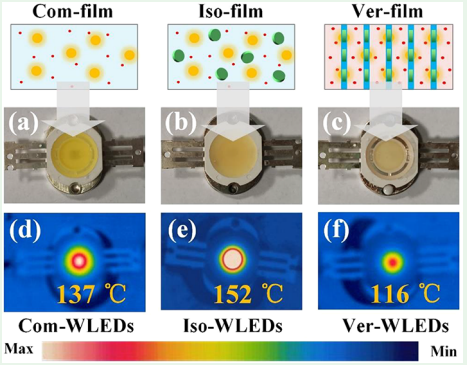


**KEYWORDS:** *LED, quantum dots, thermal conductivity, hexagon boron nitride, direction arrangement, ice-templated assembly*

## INTRODUCTION

Quantum dots (QDs) are a kind of luminescent nanocrystal semiconductor with typical dimensions of 2−20 nm. They possess prized size-, shape-, and composition-tunable electronic and optical properties due to the quantum confinement effects. Furthermore, many prospective applications can benefit from QDs' tunable properties and solution-based processing. For white-light-emitting diodes (WLEDs), QDs have been utilized to improve color quality such as color rendering index (CRI) and color saturation,[1−3] owing to their tunable emission and narrow emission line width. Specifically, the addition of red-emitting QDs to yellow-phosphor-converted WLEDs can decrease correlated color temperature (CCT) to get a warmer light and increase CRI from about 70 to larger than 90, without greatly reducing the luminous efficiency (LE).[4−7] In spite of these advantages, the thermal degradation and quenching of QDs easily happen under elevated temperatures, which seriously hinder its extensive applications in high-power quantum-dots-converted WLEDs (QDs-WLEDs). The LE of QDs decreased as temperature increased and totally and irreversibly quenched when the temperature exceeded 140 °C.[8,9] However, in high-power WLEDs for lighting application, the maximum working temperatures (MWTs) have reached up to 150−200 °C in the light converting layers.[10−12] The thermal stability issue of the QDs has become a major concern in the development of QDs-WLEDs.

To improve the thermal stability of the QDs, researchers have developed a series of solutions. Chemical modification, metal doping, and surface coating have been utilized to enlarge QDs' tolerant temperature, which inevitably resulted in a decrease of LE.[13−15] In other solutions, Zheng et al. enhanced the thermal conductivity of QDs-polymer by 40% using the electrostatic spinning technology, which reduced the working temperature from 146 to 138 °C.[16] Furthermore, Xie et al. made a compound structure of QDs and hexagonal boron nitride sheets (hBNS), which reduced the working temperature of QDs from 127.2 to 104.5 °C.[17] However, the greatest advantage of hBNS in enhancing the thermal conductivity of luminescent layer has not been used.

The hBNS have a high aspect ratio and highly anisotropic thermal property (20 W $m^{-1}$ $K^{-1}$ through plane, 585 W $m^{-1}$ $K^{-1}$ in plane for the monoisotope $^{10}B$ hBNS).[18,19] Composite materials with anisotropic thermal conductivity have been born by directionally arranging hBNS in polymers through various ways, such as magnetic field driving and ice template

**Received:** November 25, 2019
**Accepted:** December 24, 2019
**Published:** December 24, 2019






DOI: 10.1021/acsanm.9b02321
ACS Appl. Nano Mater. 2020, 3, 814−819

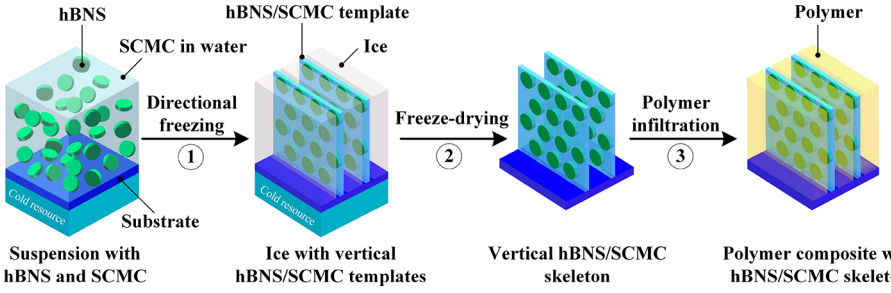


**Figure 1.** Schematic of the ice-template assembly method to generate the composite with vertically arranging hBNS.

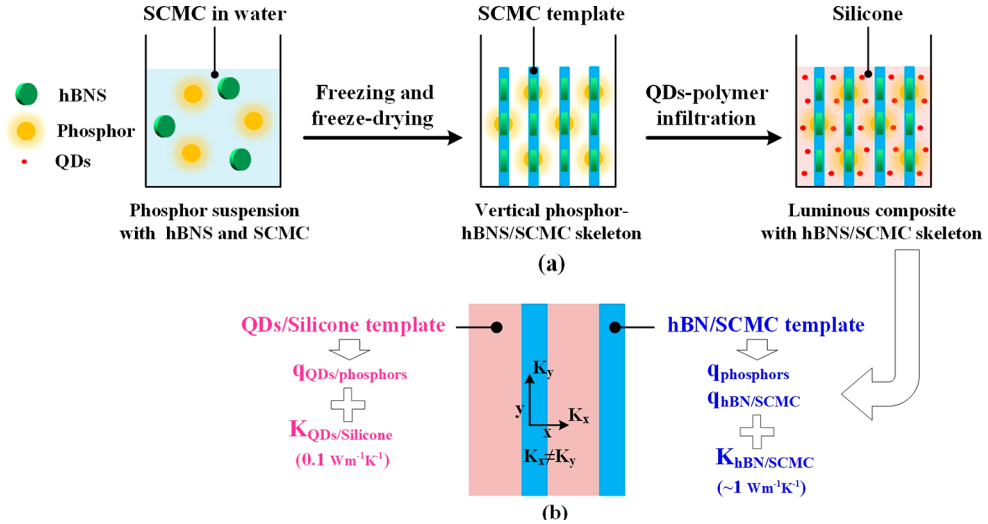


**Figure 2.** Schematics of (a) the preparation flow and (b) the thermal conduction mechanism of luminescent composite polymer with vertical hBNS/SCMC templates.

shaping.[20−25] However, the application of such materials in WLEDs is a big challenge and has not been researched, because the electoral conductivities and dark colors of the indispensable auxiliary materials such as ferroferric oxide particles and graphene oxide sheets are unacceptable in the luminescent layer of WLEDs.[20,22]

In this paper, we modified the ice templates method with an acceptable material, sodium carboxymethylcellulose (SCMC), to substitute traditional graphene oxide to connect hBNS, and thus manufactured the vertical thermal conductive QDs-WLEDs by directionally arranging hBNS in the QDs-phosphor layer. Due to the vertical thermal conduction channels made by hBNS/SCMC, heat generating from QDs and phosphors can quickly diffuse to the heat sink, avoiding the severe heat aggregation and high working temperature in the luminous layer. The following sections are the corresponding methodology, experiments, and discussion in detail.

## METHODOLOGY

Wong et al. used the growth of ice templates to shape vertical hBNS/graphene oxide templates in which graphene oxide plays an essential role in linking hBNS.[22] Our work presents an acceptable alternative material to substitute graphene oxide to connect hBNS, named sodium carboxymethylcellulose (SCMC), an industrial binder with white color and insulation properties. Figure 1 shows the schematic of the ice-template assembling progress of the composite filled with vertically arranging hBNS, including three main steps. The first step is to freeze hBNS/SCMC solution at a vertical temperature gradient, with liquid nitrogen as a cold source located on the bottom. A few minutes are needed for solution freezing to ice, and ice templates grow from the bottom to top surfaces as well as hBNS/SCMC templates. During the process of vertical crystal growth up,[26] the ice forms a large number of separated vertical ice templates, while the SCMC is squeezed into the space between the ice templates, thus forming the vertical SCMC templates. Due to the unique lamellar structure, during the crystallization process of the vertical ice templates, hBNS will be deflected under the action of torque. Until the surface is parallel to the vertical ice templates, the torque will disappear, balance will be restored, and finally hBNS will be vertically arranged in the SCMC templates. In the second freeze-drying step, the ice with vertical hBNS/SCMC templates is set in a vacuum freeze-dryer for 12 hours before the ice templates are sublimated away and the hBNS/SCMC skeleton is left. The final polymer infiltration step is to fill the vacancy in the hBNS/SCMC skeleton with luminescent composite polymer by vacuuming for 2 h.

The traditional QDs-WLEDs include blue-emitting chips, yellow-emitting phosphors (YAG:Ce), and red-emitting QDs (CdSe/CdS). It is noted that phosphors and QDs are added in various steps. The intervals between the mentioned hBNS/SCMC templates are smaller than the average diameter of yellow-emitting phosphors and larger than that of red-emitting QDs. This means that QDs can permeate into the skeleton like the polymer does but phosphors cannot. For this reason, in the preparation process shown in Figure 2a, phosphors are added in the freeze-drying solution and then evenly distributed


DOI: 10.1021/acsanm.9b02321
ACS Appl. Nano Mater. 2020, 3, 814−819

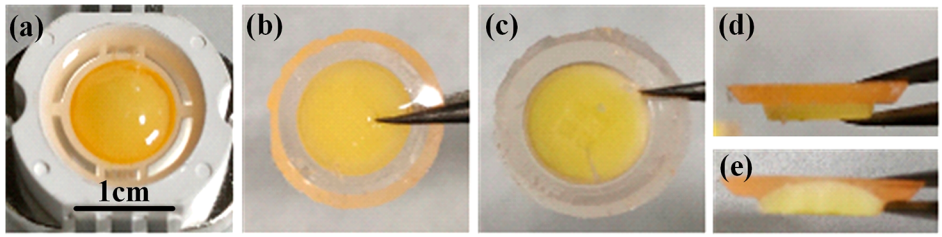


**Figure 3.** (a) Ver-WLEDs and the corresponding luminescent layer's (b) top surface, (c) lower surface, (d) lateral view, and (e) sectional view.

through the skeleton. QDs are selected to add in the silicone polymer uniformly filling the skeleton because the hydrophobic QDs will aggregate in the freeze-drying solution. Applying manufacture craft above, a novel anisotropic thermal conductive luminescent composite with vertically arranging hBNS can be prepared.

On the basis of the preparation flow in Figure 2a, the thermal conduction mechanism schematic of the anisotropic thermal conductive luminescent composite is shown in Figure 2b, including physical structure, heat source distribution, and heat conduction channels. The luminescent composite is made up by two kinds of alternate vertical arranging templates: (1) the silicone templates embedded by QDs and (2) the hBNS/SCMC templates inlayed by phosphors. The silicone and hBNS/SCMC templates feature low and high thermal conductivities, respectively. These two kinds of alternative vertical templates endow the luminous composite with a high vertical thermal conductivity and a low horizontal thermal conductivity. In addition, the main heat sources are QDs, phosphors, and hBNS/SCMC. The highly thermally conductive vertical hBNS/SCMC templates not only are the main heat diffusive channels of phosphors but also are beneficial to cool the adjacent QDs/silicone templates.

## EXPERIMENTS

On the basis of the manufacturing flow in Figure 2a, the luminous layer with vertical hBNS was coated on the surface of the chips of an LED. Vertical thermal conductive QDs-WLEDs (Ver-WLEDs) were packaged and shown in Figure 3a. The hBNS with 12 $\mu$m of average diameter and SCMC are purchased from Momentive Company and Aladdin Industrials Corporation, respectively. The luminescent layer was separated from the device and displayed in varied directions in Figure 3b–e, revealing the uniform distribution of phosphors/QDs and the complete filling of silicone. For comparison, the isotropic thermally conductive QDs-WLEDs with isotropic arranging hBNS (Iso-WLEDs) and the common QDs-WLEDs without hBNS (Com-WLEDs) were also prepared. To make a fair comparison of the LE, we adjusted the concentrations of phosphors and QDs in the above three kinds of QDs-WLEDs with similar relative spectral distributions, as shown in Table 1.

The morphologies of the SCMC, hBNS/SCMC, and hBNS/SCMC/phosphor skeleton were captured by a scanning electron microscope (SEM). The thermal diffusion coefficient of the luminescent film, $a$, was measured by a laser flash method (Netzsch LFA 457). The thermal conductivity $\lambda$ is calculated by the formula $\lambda = a\rho c$. $\rho$ and $c$ are the density and specific heat of the film. Furthermore, the temperature and spectra tests of the WLEDs were carried out by infrared photography (FLIR) and integrating sphere (Everfine, ATA-1000), respectively.

**Table 1. Different Densities of Phosphors and QDs in Three Kinds of Devices**

| | weight fractions (per gram of silicone) | | | |
|---|---|---|---|---|
| sample | phosphors | QDs | hBNS | SCMC |
| Ver-WLEDs | 2% | 0.01% | 2% | 1.5% |
| Iso-WLEDs | 2% | 0.008% | 2% | 0 |
| Com-WLEDs | 3% | 0.01% | 0 | 0 |

## RESULTS AND DISCUSSION

**Morphology.** Figure 4a,b shows the morphologies of the SCMC-based skeleton observed in the direction parallel to the SCMC templates' surface, which clearly shows the thin vertical SCMC templates. The hBNS and spherical phosphors are shown in Figure 4c,d, respectively. Seen in the perpendicular direction, as shown in Figure 4e,f, the hBNS are embedded in the SCMC templates and are almost parallel to SCMC templates. In the same observing direction, the phosphors are also embedded in the SCMC templates as shown in Figure 4g,h. It is noted that a high-volume ratio of SCMC to hBNS ensures that the skeleton does not collapse during the filling of the polymer. Meanwhile, the additions of SCMC and hBNS are limited by their negative influence on the optical performance. For balancing the structure stability and the luminous property of the luminescent composite, the concentrations of SCMC and hBNS were experimentally selected as weight fractions of 1.5% and 2%, respectively. For evaluation of the performance of vertical hBNS in the composite, the X-ray powder diffraction results of the silicone film with hBNS, the phosphor/QDs film with hBNS and SCMC, and the phosphor/QDs film with vertical hBNS/SCMC templates are shown in Figure 5. On the basis of the previous work,[19] the maximum peak, in Figure 5a, is related to the proportion of horizontal hBNS in the film. In a comparison of the marked ratios of the peak of horizontal hBNS to phosphor in Figure 5b,c, the film with vertical hBNS/SCMC templates has a relatively much lower peak from horizontal hBNS than that of the film with isotropically arranging hBNS and SCMC, which indicates the considerably larger deflection angle of hBNS resulting in vertical hBNS.

**Thermal Performance.** The luminescent films containing vertical hBNS/SCMC templates (Ver-film), with isotropic distributed hBNS (Iso-film), and without hBNS (Com-film), were made. Their thermal conductivities were tested. As shown in Figure 6a, the much higher thermal conductivities of Ver-film at varied temperatures are due to the vertical orientation of the highly thermally conductive hBNS. There are bigger error bars in the thermal conductivities of Ver-film as compared to two other kinds of films, which mainly result from the inhomogeneous interval between hBNS/SCMC templates. As shown in Figure 6b, the average thermal conductivities of Ver-film are 25% larger than those of Iso- and Com-films. It is also much higher than the thermal enhancement performance of the vertical hBNS-based polymer in the magnetic-field method, which is about 6%, in the same


DOI: 10.1021/acsanm.9b02321
ACS Appl. Nano Mater. 2020, 3, 814–819

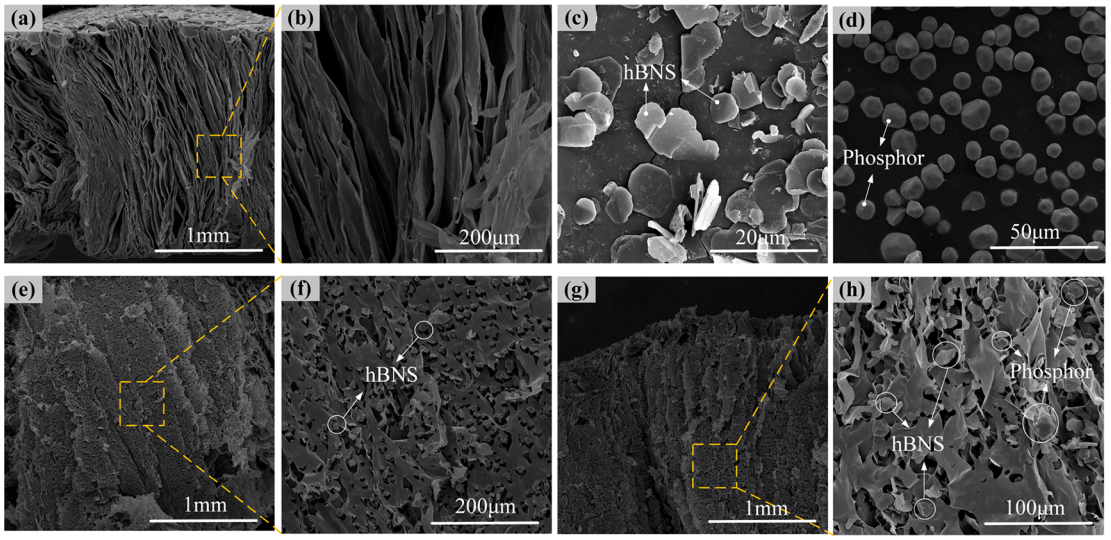


**Figure 4.** Scanning electron microscope (SEM) results of (a, b) SCMC skeleton in a direction parallel to the templates' surface, (c) hBNS, (d) phosphor, (e, f) hBNS/SCMC, and (g, h) hBNS/SCMC/phosphor skeleton in a direction perpendicular to the templates' surface.

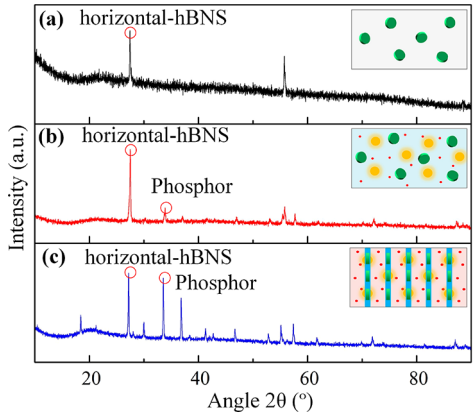


**Figure 5.** X-ray powder diffraction (XRD) results of (a) silicone film with hBNS, (b) phosphor/QDs silicone film with hBNS and SCMC, and (c) phosphor/QDs silicone film with vertical hBNS/SCMC templates.

volume ratio.[20] The higher thermal conductivity of Ver-film at 45 and 55 °C is mainly caused by the corresponding variation of the specific heat of SCMC. Moreover, we inferred the efficient thermal conductivity of the hBNS/SCMC template by efficient medium theory ($k_y = k_1 f + k_2(1 - f)$; $k_y$, $k_1$, and $k_2$ are the thermal conductivities of composite films in the $y$ direction, silicone, and hBNS/SCMC templates, respectively; $f$ is the volume fraction of silicone). On the basis of the tested thermal conductivities and the schematic of the thermal mechanism in Figure 2b, the hBNS/SCMC templates have an efficient average thermal conductivity of more than 2 W m$^{-1}$ K$^{-1}$, as the red dashed line shows in Figure 6b, nearly 20-fold that of the lateral silicone templates. Though hBNS possess fairly high thermal conductivity through the surface, the low thermal conductivity of SCMC about 0.1 W m$^{-1}$ K$^{-1}$ greatly limits the enhancement of the efficient thermal conductivity of hBNS/SCMC templates.

On the basis of the three kinds of luminescent films described above, the Ver-WLEDs, Iso-WLEDs, and Com-WLEDs were packaged. They were set in a series circuit and driven by the currents from 100 to 1000 mA. Their maximal working temperature (MWT) variations with currents are shown in Figure 7. Under the same currents, the largest and smallest MWTs were owned by the Iso- and Ver-WLEDs, respectively. Specifically, when driven by 1000 mA current, the MWTs of Com-, Iso-, and Ver-WLEDs were 137, 152, and 116 °C, respectively. In other words, compared to Com-WLEDs, the MWT of Ver-WLEDs decreased by 15%, but that of Iso-WLEDs increased by 12%. The opposite results imply one big

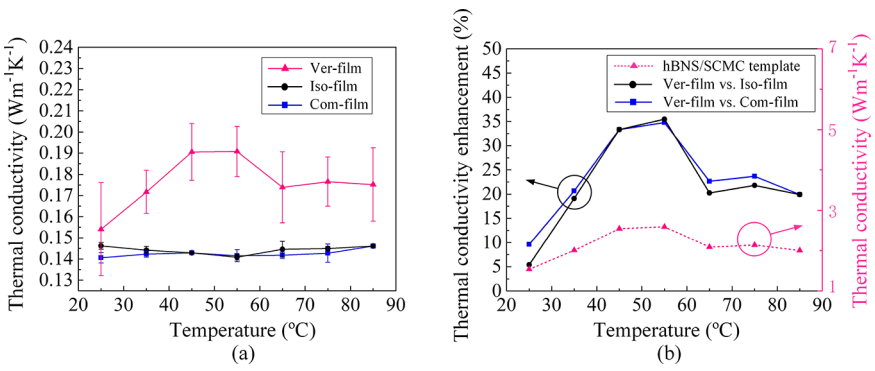


**Figure 6.** (a) Thermal conductivities of three different films: Ver-, Iso-, and Com-films. (b) Thermal conductivity enhancements of Ver-film compared to Iso- and Com-films, respectively, and the efficient thermal conductivity of hBNS/SCMC templates in the Ver-film.



DOI: 10.1021/acsanm.9b02321
ACS Appl. Nano Mater. 2020, 3, 814−819

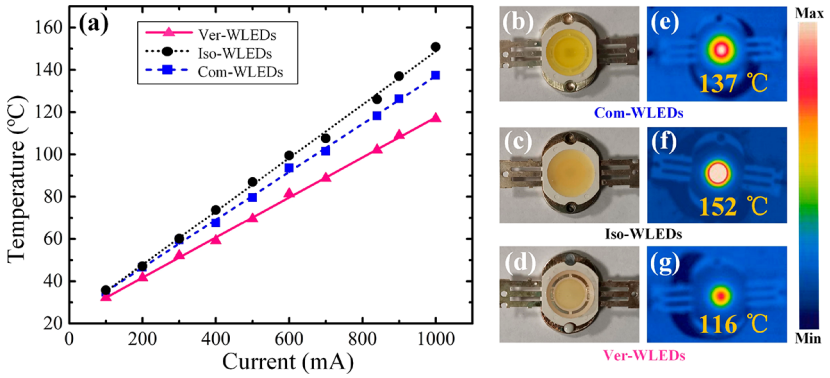


**Figure 7.** (a) Maximal working temperatures with currents. (b–d) Photos and (e–g) infrared images under working current of 1000 mA of three kinds of QDs-WLEDs.

difference between the thermal diffusion mechanisms of Ver- and Iso-WLEDs. In a comparison to Com-WLEDs, the decrease of usage of luminescent material of Iso-WLEDs and Ver-WLEDs, in Table 1, is because of the blue light loss in the luminous layer caused by hBNS and hBNS/SCMC, which means more heat loss is generated in Ver- and Iso-WLEDs, respectively. However, the isotropic thermally conductive luminescent layer in Iso-WLEDs failed to diffuse all the increased heat in time, resulting in an unexpected temperature rise. On the contrary, owing to high thermal conductivity of the vertical hBNS/SCMC templates and the special heat source distribution which have been shown in Figure 2b, the vertical thermally conductive luminescent layer in Ver-WLEDs rapidly conducted the increased heat to the heat sink, leading to a lower MWT. It is noted that, in previous work, the hBNS-adding WLEDs have smaller MWTs than common WLEDs owing to QDs being absorbed on the surfaces of hBNS for heat diffusion.[17] However, in this work, QDs and hBNS are separated in the luminous layer of Iso-WLEDs. Despite the enhancement of thermal conductivity of the luminous layer of Iso-WLEDs, the heat loss caused by hBNS still leads to a higher MWT than that of Com-WLEDs.

**Optical Performance.** The relative luminescent spectra of three kinds of QDs-WLEDs were tested under 1000 mA direct current, as shown in Figure 8a. To ensure the consistency of the relative spectra, all the samples generated similar high-quality light with CCT of about 6000 K and CRI of about 85. However, the LE values of each other varied: the LE of Ver-WLEDs (49.4 lm/W) was 15% and 29% less than those of Iso-WLEDs (58.1 lm/W) and Com-WLEDs (70.0 lm/W), respectively. This is mainly because of the inevitable light absorption effects of SCMC and hBNS, and guided trapping effects of SCMC and scattering effects of hBNS. Figure 8b shows the effect of the hBNS/SCMC skeleton on the spectra of the luminescent layers with only phosphors or QDs. Although the yellow light from the phosphors was maintained in the phosphors/hBNS/SCMC case and the red light from the QDs even increased in the QDs/hBNS/SCMC case, the light converting efficiencies are both reduced, owing to the blue light absorption and loss caused by hBNS/SCMC. In addition, the blue light reduction of the phosphor and QD cases is larger than that of the silicone case, because phosphors and QDs enhanced the scattering of blue light and thus caused more light loss.

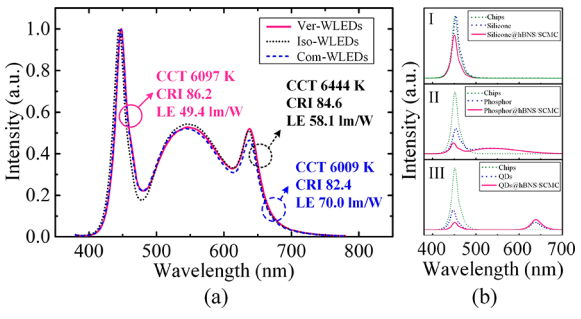


**Figure 8.** (a) Relative luminescent spectra of three kinds of QDs-WLEDs. (b) Luminescent spectra effects of hBNS/SCMC skeleton on silicone, phosphors, and QDs-added silicone.

## CONCLUSION

The thermal stability of QDs is challenged by the high working temperature of the luminescent polymer layer with a low thermal conductivity in QDs-WLEDs. In this work, we proposed a new package process of QDs-WLEDs. This had a relatively high vertical thermal-conductivity luminescent layer filled with vertically arranging hBNS using an ice template method, so that a high thermal conductivity heat dissipation channel was created for luminescent particles. Experimental results showed that the MWT of Ver-WLEDs (116 °C) was 36 and 21 °C smaller than those of Iso-WLEDs (152 °C) and Com-WLEDs (137 °C), respectively. In addition, the LE of Ver-WLEDs decreased, but the CRI and CCT were maintained. Our novel method to enhance the vertical thermal conductivity of the luminescent polymer layer can broaden the application of temperature-dependent unstable QDs in high-power WLEDs.

## AUTHOR INFORMATION


### Corresponding Authors

*E-mail: luoxb@hust.edu.cn.

*E-mail: wangk@sustc.edu.cn.

### ORCID

Kai Wang: 0000-0003-0443-6955

Xiaobing Luo: 0000-0002-6423-9868


### Notes

The authors declare no competing financial interest.

## ACKNOWLEDGMENTS

The authors would like to acknowledge the financial support by National Natural Science Foundation of China (51625601, 51576078, 51606074, and 61875082), the Ministry of Science



DOI: 10.1021/acsanm.9b02321
ACS Appl. Nano Mater. 2020, 3, 814–819

and Technology of the Peoplés Republic of China (2017YFE0100600, 2017YFE0120400), Creative Research Groups Funding of Hubei Province (2018CFA001), Natural Science Foundation of Guangdong (No.2017B030306010), and Shenzhen Innovation Project (JSGG20170823160757004).

## REFERENCES

(1) Chen, O.; Wei, H.; Maurice, A.; Bawendi, M.; Reiss, P. Pure Color from Core-Shell Quantum Dots. *MRS Bull.* **2013**, *38*, 696−702.
(2) Kim, S.; Im, S. H.; Kim, S.-W. Performance of Light-Emitting-Diode Based on Quantum Dots. *Nanoscale* **2013**, *5* (12), 5205−5214.
(3) Zhu, R.; Luo, Z.; Chen, H.; Dong, Y.; Wu, S.-T. Realizing Rec. 2020 Color Gamut with Quantum Dot Displays. *Opt. Express* **2015**, *23* (18), 23680.
(4) Nizamoglu, S.; Zengin, G.; Demir, H. V. Color-conversion Combinations of Nanocrystal Emitters for Warm-White Light Generation with High Color Rendering Index. *Appl. Phys. Lett.* **2008**, *92* (3), 031102.
(5) Hong, Q.; Lee, K. C.; Luo, Z.; Wu, S. T. High-efficiency Quantum Dot Remote Phosphor Film. *Appl. Opt.* **2015**, *54* (15), 4617−4622.
(6) Woo, J. Y.; Kim, K.; Jeong, S.; Han, C.-S. Enhanced Photoluminance of Layered Quantum Dot-Phosphor Nanocomposites as Converting Materials for Light Emitting Diodes. *J. Phys. Chem. C* **2011**, *115*, 20945−20952.
(7) Xie, B.; Hu, R.; Luo, X. Quantum Dots-converted Light-Emitting Diodes Packaging for Lighting and Display: Status and Perspectives. *J. Electron. Packag.* **2016**, *138* (2), 020803.
(8) Woo, J. Y.; Kim, K. N.; Jeong, S.; Han, C.-S. Thermal Behavior of a Quantum Dot Nanocomposite as a Color Converted Material and Its Application to White LED. *Nanotechnology* **2010**, *21*, 495704.
(9) Zhao, Y.; Riemersma, C.; Pietra, F.; Koole, R.; de Mello Donega, C.; Meijerink, A. High-temperature Luminescence Quenching of Colloidal Quantum Dots. *ACS Nano* **2012**, *6* (10), 9058−9067.
(10) Bachmann, V. M.; Ronda, C.; Meijerink, A. Temperature Quenching of Yellow Ce3+ Luminescence in YAG:Ce. *Chem. Mater.* **2009**, *21* (10), 2077−2084.
(11) Ma, Y.; Lan, W.; Xie, B.; Hu, R.; Luo, X. An Optical-thermal Model for Laser-excited Remote Phosphor with Thermal Quenching. *Int. J. Heat Mass Transfer* **2018**, *116*, 694−702.
(12) Peng, Y.; Mou, Y.; Sun, Q.; Cheng, H.; Chen, M.; Luo, X. Facile Fabrication of Heat-conducting Phosphor-in-glass with Dual-sapphire Plates for Laser-driven White Lighting. *J. Alloys Compd.* **2019**, *790*, 744−749.
(13) Tomczak, N.; Janczewski, D.; Han, M. Y.; Vancso, G. J. Designer Polymer-quantum Dot Architectures. *Prog. Polym. Sci.* **2009**, *34*, 393−430.
(14) Zhao, B.; Yao, X.; Gao, M.; Sun, K.; Zhang, J.; Li, W. Doped Quantum Dot Silica Nanocomposites for White Light-emitting Diodes. *Nanoscale* **2015**, *7*, 17231−17236.
(15) Selvan, S. T.; Tan, T. T.; Ying, J. Y. Robust, Non-cytotoxic, Silica-coated Cdse Quantum Dots with Efficient Photoluminescence. *Adv. Mater.* **2005**, *17* (13), 1620−1625.
(16) Zheng, H.; Lei, X.; Cheng, T.; Liu, S.; Zeng, X.; Sun, R. Enhancing the Thermal Dissipation of a Light-conversion Composite for Quantum Dot-based White Light-emitting Diodes Through Electrospinning Nanofibers. *Nanotechnology* **2017**, *28*, 265204.
(17) Xie, B.; Liu, H.; Hu, R.; Wang, C.; Hao, J.; Wang, K.; Luo, X. Targeting Cooling for Quantum Dots in White QDs-LEDs by Hexagonal Boron Nitride Platelets with Electrostatic Bonding. *Adv. Funct. Mater.* **2018**, *28*, 1801407.
(18) Zhang, K.; Feng, Y.; Wang, F.; Yang, Z.; Wang, J. Two Dimensional Hexagonal Boron Nitride (2D-hBN): Synthesis, Properties and Applications. *J. Mater. Chem. C* **2017**, *5*, 11992−12022.
(19) Yuan, C.; Li, J.; Lindsay, L.; Cherns, D.; Pomeroy, J. W.; Liu, S.; Edgar, J. H.; Kuball, M. Modulating the Thermal Conductivity in Hexagonal Boron Nitride via Controlled Boron Isotope Concentration. *Commun. Phys.* **2019**, *2*, 43.
(20) Yuan, C.; Duan, B.; Li, L.; Xie, B.; Huang, M.; Luo, X. Thermal Conductivity of Polymer-based Composites with Magnetic Aligned Hexagonal Boron Nitride Platelets. *ACS Appl. Mater. Interfaces* **2015**, *7*, 13000−13006.
(21) Yuan, J.; Qian, X.; Meng, Z.; Yang, B.; Liu, Z. Highly Thermally Conducting Polymer-based Films with Magnetic Field-assisted Vertically Aligned Hexagonal Boron Nitride for Flexible Electronic Encapsulation. *ACS Appl. Mater. Interfaces* **2019**, *11* (19), 17915−17924.
(22) Zeng, X.; Yao, Y.; Gong, Z.; Wang, F.; Sun, R.; Xu, J.; Wong, C. P. Ice-templated Assembly Strategy to Construct 3D Boron Nitride Nanosheet Networks in Polymer Composites for Thermal Conductivity Improvement. *Small* **2015**, *11* (46), 6205−6213.
(23) Yao, Y.; Sun, J.; Zeng, X.; Sun, R.; Xu, J. B.; Wong, C. P. Construction of 3D Skeleton for Polymer Composites Achieving a High Thermal Conductivity. *Small* **2018**, *14* (13), 1704044.
(24) Bo, Z.; Ying, C.; Zhu, H.; Wei, X.; Yang, H.; Yan, J.; Cen, K. Bifunctional Sandwich Structure of Vertically-oriented Graphenes and Boron Nitride Nanosheets for Thermal Management of LEDs and Li-ion Battery. *Appl. Therm. Eng.* **2019**, *150*, 1016−1027.
(25) Han, J.; Du, G.; Gao, W.; Bai, H. An Anisotropically High Thermal Conductive Boron Nitride/epoxy Composite Based on Nacre-mimetic 3D Network. *Adv. Funct. Mater.* **2019**, *29* (13), 1900412.
(26) Deville, S.; Saiz, E.; Nalla, R. K.; Tomsia, A. P. Freezing as a Path to Build Complex Composites. *Science* **2006**, *311* (5760), 515−518.



DOI: 10.1021/acsanm.9b02321
*ACS Appl. Nano Mater.* 2020, 3, 814−819